Comparison of Noise-Parameter Measurement Strategies: Simulation Results for Amplifiers*

James Randa

RF Technology Division

National Institute of Standards and Technology (NIST)

Boulder, CO 80303

Abstract — A previously developed simulator for noise-parameter measurements has been used in an extensive investigation and comparison of different measurement strategies for measuring the noise parameters of low-noise amplifiers (LNAs). This paper summarizes the methodology and reports the salient results of that investigation. The simulator is based on a Monte Carlo program for noise-parameter uncertainties and enables us to compare the uncertainties (both type A and type B) obtained with a given set of input terminations. We focus on results that do not depend (or depend only weakly) on details of the device under test (DUT). One noteworthy result is the marked improvement in the noise-parameter measurement uncertainties when a matched, cold (*i.e.*, well below ambient noise temperature) source is included in the set of input terminations.

Index Terms — Amplifier noise measurement, amplifier noise parameters, noise-parameter measurement, measurement uncertainty, Monte Carlo simulation.

I. Introduction

Several years ago, a simulator for noise-parameter measurements was developed [1], based on a Monte Carlo program for noise-parameter uncertainties [2]. Some minor improvements have been made to that simulator, and it has now been used in a rather extensive investigation and comparison of different strategies for measuring the noise parameters of low-noise amplifiers (LNAs). This paper summarizes the methodology and reports the salient results of that investigation. We focus on results that do not depend (or depend only weakly) on details of the device under test (DUT).

There is commercial instrumentation that enables the user to perform routine amplifier noise-parameter measurements, but it is still of interest to consider how such measurements might be improved, or what strategies might be employed for difficult special cases. Some of the results might be anticipated based on common intuition, but even in such cases it is still useful to have a quantitative confirmation and an estimate of the size of the expected effect. In this paper, we compare different measurement strategies on the basis of the uncertainties obtained with the given strategy (or set of input states) and on the basis of the frequency of occurrence of unphysical measurement results or sets of measurements that do not admit a good fit to the simulated measurement data.

From the early days of noise-parameter measurements, there has been work on choosing the set of input terminations; see, *e.g.*, [3] – [5] or the summary in [6]. The present investigation assumes that the specific properties of the DUT are not known, although its general characteristics may be. We do not attempt to find the optimum pattern of impedances for the input terminations for a given amplifier. Instead, we try to find general features of the input set that work well for a range of amplifiers. We also consider variations in the measurement strategy, such as inclusion of additional non-ambient inputs or inclusion of a reverse measurement.

In our simulations, we start with a basic measurement strategy, with a small set of input states, and consider a number of possible improvements. Some of the improvements are modifications of the input states, adding or substituting additional states, and some involve modifications of the basic measurement set. Of course, the results depend on details of the amplifier being measured. In order to identify general features that are likely to be true for most DUTs, we have performed all the simulations on three different amplifiers, with very different properties.

In the next section we provide a short overview of the simulator, including the input uncertainties and the recent modification. We also give the properties of the amplifiers and input terminations that we consider in this work. Section III presents the simulations performed and the results obtained, and Section IV contains a summary and conclusions.

II. Methodology

A. The Simulator

The simulator assumes measurements of the form pictured in Figure 1, which also shows relevant conventions regarding notation. The DUT is characterized by its scattering parameters (S_{ij}) and its noise parameters. A series of input terminations with known noise temperatures ($T_{1,i}$) and reflection coefficients ($\Gamma_{1,i}$) is connected to the input of the DUT, and the output noise temperature ($T_{2,i}$) or noise power is

*

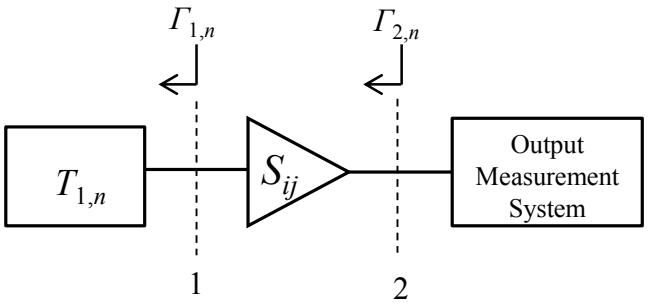

Fig. 1 Configuration for forward measurements.

measured for each. An equation can be written for the output noise temperature (or noise power) as a function of the four noise parameters and the gain, and the noise parameters and gain can then be determined by fitting to the set of equations for the output for each different input termination. There are many different, equivalent forms for the equations [6]; we perform the analysis and computations in terms of noise-wave parameters, but we will present and discuss the results in terms of the usual IEEE noise parameters.

For a given measurement strategy and set of input terminations, the simulation program generates N_S sets of simulated measurements. All results reported in this paper were obtained with N_S = 20,000. Each set includes all input noise temperatures and reflection coefficients, the amplifier S-parameters, the output noise temperatures, and the output reflection coefficients $\Gamma_{2,n}$. (The output reflection coefficients can instead be computed from input reflection coefficients and S-parameters; see subsection III.E below.) Each simulated measurement set is analyzed in the same manner as a real set of measurements would be analyzed, with a least-squares fit to the set of equations for the output noise temperature in terms of the noise parameters (and the measured quantities). The fit results in values for each noise parameter (and the gain), as well as a type A uncertainty for each of these quantities, which is obtained from the statistics of the fit. The type B uncertainty is computed in the usual Monte Carlo manner, taking the root mean square error (RMSE) of the sample of N_S values,

$$u_B(y) = RMSE(y) = \sqrt{Var(y) + (\bar{y} - y_{true})^2}, \qquad (1)$$

where y is any of the noise parameters, and $Var(y)$ is the variance of the sample of simulated results for y. The fact that the mean ($\bar{y}$) is not necessarily equal to the "true" value is due to the presence of various nonlinearities. In order to obtain a representative value of the type A uncertainty for the particular measurement strategy that we are considering, we take the root mean square of the N_S values for the type A uncertainty in that noise parameter.

Some quality checks (goodness of fit, physical and mathematical consistency of results) are applied to each set of simulated measurement results, as would be done for real results [6]. A measurement set that fails one or more of these tests is considered a "bad" set and is discarded (as is usually the case for real measurements), and it is not included in the computation of uncertainties. The different measurement strategies are compared and judged on the basis of the frequency of occurrence of bad results, as well as the standard uncertainties (type A and type B added in quadrature) obtained for the noise parameters. Results that differ by a few percent or less are not significant; differences of more than about 5 % are significant.

B. Input Uncertainties

The simulation program accepts as input not only the values of the all the parameters, but also the standard uncertainties in the parameters that are directly measured, including the DUT S-parameters, the reflection coefficients of all the terminations, the noise temperatures of all the terminations, the output reflection coefficients $\Gamma_{2,n}$ in Fig. 1, and the output noise temperatures. We refer to the uncertainties in these underlying measurements as the input uncertainties. Although the values obtained for the noise-parameter uncertainties will depend on the input uncertainties, we will concentrate on whether the uncertainties are significantly improved by a given measurement strategy, rather than on the actual values of the uncertainties. Nonetheless, we need to specify the input uncertainties.

Most of the input uncertainties are those used in [2], which also discusses the reasoning behind the values chosen. In treating correlations, which are of crucial importance, we work in terms of correlated and uncorrelated uncertainties, defined by the relations

$$u(y_i)^2 = u_{unc}(y_i)^2 + u_{cor}(y_i)^2$$

$$\rho_{ij} = \frac{u_{cor}(y_i)u_{cor}(y_j)}{u(y_i)u(y_j)}, \qquad (2)$$

where "*cor*" and "*unc*" refer to correlated and uncorrelated, and ρ_{ij} is the correlation coefficient for errors in y_i and y_j. Normal distributions are used for all the measured variables except the ambient temperature, for which a rectangular distribution is used, in order to more accurately represent the effect of thermostatic control.

The real and imaginary parts of the reflection coefficient are treated separately, and the same $u(\Gamma)$ is used for each, where $u(\mathrm{Re}\Gamma) = u(\mathrm{Im}\Gamma) \equiv u(\Gamma)$. For reflection-coefficient measurements, a larger value of uncertainty is used for large $|\Gamma|$ than for small $|\Gamma|$. For $|\Gamma| \le 0.5$, we use $u_{cor} = 0.0025$ and $u_{unc} = 0.001$, corresponding to $u(\Gamma) = 0.002693$ and $\rho = 0.8621$. For larger values of $|\Gamma|$, we use $u_{cor} = 0.004$ and $u_{unc} = 0.001$, corresponding to $u(\Gamma) = 0.004123$ and $\rho = 0.9412$. All S-parameters other than S_{21} are treated the same way as reflection coefficients. The value used for S_{21} is not very important because its magnitude is treated as a fitting parameter, $G_0 = |S_{21}|^2$; we use $u(\mathrm{Re}S_{21}) = u(\mathrm{Im}S_{21}) = 0.01$.

For the ambient temperature we use a rectangular distribution centered at the nominal laboratory temperature of 296.15 K, extending from 295.65 K to 296.65 K, with no correlation between separate measurements (since a considerable time period intervenes between separate measurements). For the noise temperatures of the input terminations, we use a fractional uncertainty of 0.005 for hot or cold terminations. For ambient or near-ambient (*i.e.*, within 20 K of ambient) terminations, we use the uncertainty in the ambient temperature.

One departure from the previous input uncertainties occurs for the measurement of output noise temperatures. In the past, we used a simple parameterization depending only on the value of the noise temperature being measured, unless an adapter was present. That parameterization relied on the output reflection coefficient not being too large. In order to treat poorly matched amplifiers, we have modified the uncertainty in measuring the output noise temperatures to include more details of the DUT and the measurement process. The new model includes estimates of the five principal contributions to noise-temperature measurement uncertainties (at least at NIST): the cryogenic standard, the ambient standard, the evaluation of the mismatch factor(s), the ratio of efficiencies for the different measurement paths, and the instrument linearity. These five contributions are combined in quadrature to yield the standard uncertainty. For large output reflection coefficients, the new model yields a somewhat larger value for the measurement uncertainty than did the previous model.

C. LNAs and Input States

We do not want our results to depend on specific features of the DUT, but on the other hand, the simulator requires specific values for the DUT scattering and noise parameters. We therefore apply each measurement strategy to three different amplifiers, whose properties span a wide range of values of interest. We label the three amplifiers A1, A2, and A3. Their scattering and noise parameters are given in Tables 1 and 2. (Phases of *S*-parameters are omitted to save space.) Amplifier A1 has a low noise figure, A3 has a high noise figure, and A2 lies between. A1 and A2 have gains in the range of 32 dB to 33 dB, whereas A3 has lower gain, around 23 dB. A1 and A2 are reasonably well matched, but A3 has $|S_{11}| \approx 0.47$. All three amplifiers have $|\Gamma_{opt}|$ around 0.2. All three sets of properties are realistic in the sense that they were obtained in measurements on real amplifiers in the 1 – 12 GHz range.

Table 1. DUT *S*-parameters (to three significant places).

DUT	$\|S_{11}\|$	$\|S_{12}\|$	$\|S_{21}\|$	$\|S_{22}\|$
A1	0.248	0.00245	41.3	0.181
A2	0.180	0.0005	43.5	0.113
A3	0.469	0.0041	14.6	0.127

Table 2. DUT noise parameters (to three significant places).

DUT	G_0	$T_{e,min}$(K)	R_n(Ω)	$\|\Gamma_{opt}\|$	φ_{opt} (degr)	F_{min} (dB)
A1	1740	59.7	6.55	0.199	35.3	0.813
A2	1890	115	5.68	0.194	151	1.112
A3	220	291	19.8	0.226	91.8	3.021

We must also specify the input terminations to be used. Most of the strategies considered below differ in the set of input terminations used. Figure 2 plots the location in the complex plane of the reflection coefficients of the terminations used in this study, with labels to allow convenient reference. There are eight highly reflective terminations (R1 – R8), seven less reflective terminations (R1' – R7'), six "interior" points (I1 – I6), and four nearly reflectionless loads clustered around the origin—one ambient (a), two hot (h1, h2), and one cold (c). Unless otherwise specified, all the R, R', and I terminations have ambient noise temperature. Most of our results will concern the efficacy of using various sets of input terminations (or input states) in the noise-parameter measurements.

III. Simulations and Results

A. Base Configuration(s)

In order to establish a baseline for comparing the results obtained with different strategies, we choose a base set of input states, which will be labelled "B." Since we are fitting for five parameters (four noise parameters plus G_0), at least five different input states are required. At least one additional state is required if we are to have meaningful type A uncertainties. Because we are including G_0 in the fitting parameters, we need at least two different input noise tempera-

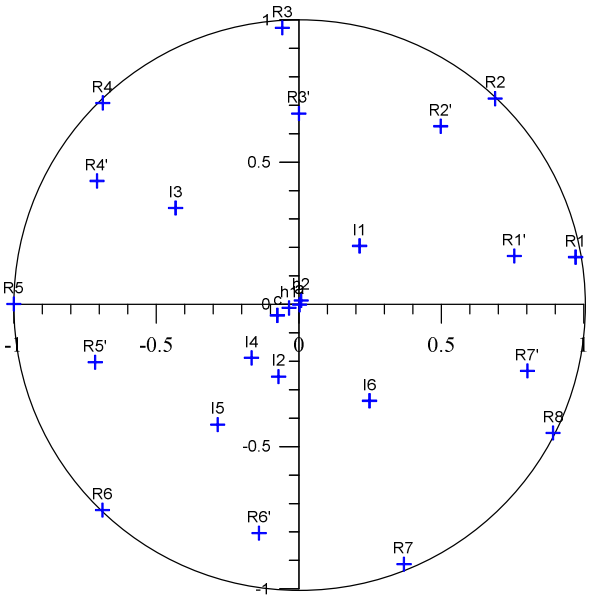

Fig. 2 Reflection coefficients of input states used in study.

tures. The base set that we choose consists of B = {a, h1, R1, R3, R5, R7}, *i.e.*, one ambient and one hot matched load plus four highly reflective terminations. In principle, it is possible that these specific reflection coefficients could conspire with the particular noise parameters that we have chosen and "accidentally" yield especially good or bad results that were not representative of the general situation. To guard against that possibility, we also consider a second base set B2 = {a, h1, R2, R4, R6, R8} and check that results obtained with B and with B2 are not dramatically different.

Simulation results obtained with input sets B and B2 for the three amplifiers A1, A2, and A3 are summarized in Table 3. We have shown results for the IEEE parameters and for magnitude and phase of Γ_{opt}, since they are probably the most familiar. It is clear that the results are consistent, and therefore fears that we have accidentally chosen special values or states for B are unfounded. In Table 3 all uncertainties are standard uncertainties (1 σ), and BadFrac is the fraction of the simulated measurement sets that produced bad results, either a poor fit for the noise parameters or a violation of one or more physical or mathematical constraints, as mentioned in II.A. The rather large values for BadFrac, particularly for A1, may be somewhat unsettling. Note that A1 is a rather challenging device to measure, with high gain and low noise temperature, and the base sets contain fewer input terminations than would normally be used. It is also possible that the input uncertainties that we use are more conservative than is necessary or realistic. For purposes of this study, however, what is important is not actual value of BadFrac, but whether it is better or worse for different sets of input states or different measurement strategies.

B. Other Non-Ambient Matched Loads

We first consider the choice of the non-ambient matched load(s). The noise temperature of the hot load h1 in the base set is 1232 K, which is a typical temperature for a hot load in such measurements. We have run simulations using a cryogenic load (c, noise temperature T_c = 99 K) either in place of or in addition to h1. We have also considered cooler (h2, T_{h2} = 750 K) and hotter (h3, T_{h3} = 5000 K) hot loads and various combinations of h1, h2, h3, and c. Some results of those simulations are given in Table 4. In the entries under "Input," B represents the base set, a minus sign indicates that the following state was removed from B, and a plus sign indicates that the following state was added to B. Thus, for example, B-h1+c represents an input state consisting of B without h1 but with c, *i.e.*, the set {a, c, R1, R3, R5, R7}.

Many effects can be gleaned from a detailed examination of Table 4. We will note only the most salient. Changes of the non-ambient input state(s) have a negligible effect on uncertainties in Γ_{opt}. Not surprisingly, the biggest effects are on the determination of G_0 and T_{min}. For amplifiers whose value of T_{min} is significantly below T_{amb}, using the cold input termination c instead of the hot termination h1 results in a significant reduction in the uncertainty in T_{min}, accompanied by a small increase in $u(G_0)$. Using the cold input in addition to h1 results in major improvements in $u(T_{min})$ (more than a factor of two for A1 and A2) and a small improvement in

Table 3. Comparison of results for two different base sets.

DUT Input	Bad Frac	$u(G_0)$	$u(T_{min})$ (K)	$u(R_n)$ (Ω)	$u(\lvert\Gamma_{opt}\rvert)$	$u(\varphi_{opt})$
A1						
B	0.35	17.8	4.1	0.091	0.0093	0.61
B2	0.34	17.7	4.1	0.088	0.0091	0.61
A2						
B	0.16	19.6	4.7	0.080	0.0048	0.40
B2	0.18	19.6	4.7	0.080	0.0048	0.41
A3						
B	0.17	2.5	7.5	0.23	0.0044	0.12
B2	0.17	2.5	7.4	0.22	0.0039	0.13

Table 4. Simulation results for different non-ambient input noise sources.

DUT Input	Bad Frac	$u(G_0)$	$u(T_{min})$ (K)	$u(R_n)$ (Ω)	$u(\lvert\Gamma_{opt}\rvert)$	$u(\varphi_{opt})$
A1						
B	0.35	17.8	4.1	0.091	0.0093	0.61
B-h1+c	0.35	18.8	2.3	0.091	0.0093	0.61
B-h1+h2	0.35	22.5	5.2	0.105	0.0093	0.61
B-h1+h3	0.35	14.8	3.2	0.083	0.0093	0.61
B+c	0.30	13.6	1.8	0.080	0.0094	0.62
B+h2	0.39	16.0	4.0	0.088	0.0094	0.62
B+h2+c	0.34	12.3	1.7	0.078	0.0095	0.62
A2						
B	0.16	19.6	4.7	0.080	0.0048	0.40
B-h1+c	0.16	22.6	3.1	0.084	0.0048	0.40
B-h1+h2	0.16	25.1	6.0	0.093	0.0048	0.40
B-h1+h3	0.16	15.9	3.6	0.072	0.0048	0.40
B+c	0.15	15.4	2.2	0.071	0.0049	0.41
B+h2	0.25	17.7	4.6	0.077	0.0049	0.41
B+h2+c	0.20	13.9	2.0	0.069	0.0049	0.41
A3						
B	0.17	2.5	7.5	0.23	0.0044	0.12
B-h1+c	0.17	3.9	8.2	0.35	0.0044	0.12
B-h1+h2	0.17	3.3	10.2	0.31	0.0044	0.12
B-h1+h3	0.17	1.9	5.5	0.17	0.0044	0.12
B+c	0.14	2.1	4.6	0.19	0.0045	0.13
B+h2	0.22	2.3	7.5	0.22	0.0045	0.13
B+h2+c	0.17	1.9	4.3	0.17	0.0045	0.13

$u(G_0)$. In general, the higher the noise temperature of the hot source, the smaller are the uncertainties in G_0 and T_{min}. Using a cold input source in addition to the hot source is a clear recommendation, particularly since it is not particularly difficult (if a cold noise source is available). Because of the input uncertainties used for the input noise sources, the cold input noise source c is assumed to be a calibrated synthetic noise source (see, *e.g.*, [7] – [9]), rather than a cryogenic standard.

C. Additional Reflective Terminations

We next turn our attention to the question of whether it is useful to include additional reflective terminations. The results depend to some extent on the reflection coefficient(s) of the additional terminations and the properties of the amplifiers, so we have done the following. Starting with the base set B, we added one reflective termination R2 and performed the simulations on B+R2. We then added a different reflective termination R4 and obtained results for B+R4. This was done for each of the four resistive terminations not already included in B, that is, for R2, R4, R6, and R8. We averaged the results of those four sets of simulations to get representative results for adding one additional reflective termination. We then repeated the process adding two reflective terminations at a time, in all possible combinations, and averaging them, and then doing the same for three additional terminations. Finally, we added all four additional terminations, B+B2. Results are tabulated in Table 5, where we have used B+1R to represent the average of the results with one reflective termination added to B, etc.

The effect of adding additional reflective terminations is not very dramatic. It has no significant effect on the uncertainties in R_n or Γ_{opt}; and for G_0, T_{min}, and BadFrac, the effect is small or insignificant. Although the effect is small for these three quantities, it warrants some discussion because it is rather counter-intuitive. In some cases (highlighted entries in Table 5), adding one or more additional reflective terminations seems to make matters worse, albeit by a small amount. This effect is the result of two features of the computations. The principal cause is probably the fact that we are adding terminations with reflection coefficients that are very close to the edge of the unit circle compared to the uncertainty in measuring them, and the calculations are quite sensitive to these reflection coefficients, due to the occurrence of factors like $(1-|\Gamma|^2)^{-1}$. A simple check of this explanation is to reduce the relevant input uncertainties and see whether that reduces or removes the peculiar results. We performed that test, and it confirms the explanation. As a further check, we have performed the simulations using terminations that were somewhat less reflective, and again the peculiar results disappeared. We should also remember that the simulated measurement sets with "bad" results contribute to BadFrac, but they are excluded from the uncertainty computations.

Table 5. Simulation results with added reflective terminations.

DUT Input	Bad Frac	$u(G_0)$	$u(T_{min})$ (K)	$u(R_n)$ (Ω)	$u(\lvert\Gamma_{opt}\rvert)$	$u(\varphi_{opt})$
A1						
B	0.35	17.8	4.1	0.091	0.0093	0.61
B+1R	0.38	18.6	4.3	0.093	0.0093	0.61
B+2R	0.40	18.8	4.4	0.093	0.0092	0.61
B+3R	0.42	19.2	4.5	0.093	0.0091	0.60
B+4R	0.44	19.4	4.6	0.093	0.0090	0.59
A2						
B	0.16	19.6	4.7	0.080	0.0048	0.40
B+1R	0.16	20.3	4.9	0.081	0.0048	0.40
B+2R	0.14	20.5	5.0	0.082	0.0048	0.40
B+3R	0.13	20.8	5.1	0.081	0.0047	0.40
B+4R	0.12	21.0	5.1	0.081	0.0047	0.40
A3						
B	0.17	2.5	7.5	0.23	0.0044	0.12
B+1R	0.14	2.6	7.8	.23	0.0043	0.12
B+2R	0.11	2.6	8.0	.23	0.0043	0.12
B+3R	0.090	2.6	8.1	.24	0.0042	0.12
B+4R	0.078	2.6	8.2	.24	0.0041	0.11

Therefore, we exclude some of the simulated measurements with the largest errors.

In view of the simulation results and the preceding discussion, we conclude that with our input uncertainties, the inclusion of additional reflective terminations in the input set leads to no significant improvement in the measurement uncertainties or the fraction of bad measurements.

D. Additional Interior Points

So far, the only input states that we have considered have been either highly reflective or nearly matched. Most practical measurements also include input reflection coefficients distributed in the interior of the unit circle. We have run simulations with input sets that included one or more interior (but not matched) reflection coefficients (I1 – I6 in Fig. 2). Results are tabulated in Table 6. In a similar manner as was done for the reflective terminations, we use B+1I to refer to the results obtained by adding one interior point to the base set, averaged over four different choices (I1, I3, I5, I6) for the additional interior terminations. B+2I refers to the inclusion of two interior points, etc. The results of Table 6 indicate that there is a significant benefit to including several interior points among the input terminations. Because of our imposition of the various checks, the benefit is manifest primarily as a decrease in the occurrence of bad measurements. We conclude that there is good reason for the common practice of having

Table 6. Simulation results with added interior terminations.

DUT Input	Bad Frac	$u(G_0)$	$u(T_{min})$ (K)	$u(R_n)$ (Ω)	$u(\lvert\Gamma_{opt}\rvert)$	$u(\varphi_{opt})$
A1						
B	0.35	17.8	4.1	0.091	0.0093	0.61
B+1I	0.26	18.2	3.9	0.093	0.0094	0.62
B+2I	0.21	18.3	3.8	0.094	0.0094	0.62
B+3I	0.17	18.4	3.8	0.094	0.0096	0.62
B+4I	0.14	18.5	3.8	0.094	0.0095	0.63
A2						
B	0.16	19.6	4.7	0.080	0.0048	0.40
B+1I	0.12	20.1	4.5	0.081	0.0048	0.40
B+2I	0.090	20.1	4.4	0.081	0.0048	0.41
B+3I	0.070	20.2	4.3	0.081	0.0049	0.41
B+4I	0.058	20.4	4.3	0.081	0.0049	0.41
A3						
B	0.17	2.5	7.5	0.23	0.0044	0.12
B+1I	0.12	2.5	7.2	0.23	0.0044	0.13
B+2I	0.081	2.5	7.1	0.23	0.0045	0.13
B+3I	0.057	2.5	6.9	0.23	0.0045	0.13
B+4I	0.042	2.5	6.9	0.23	0.0045	0.13

input reflection coefficients distributed throughout the unit circle (or across the Smith chart).

E. Reverse Measurements

Various authors have suggested direct measurement of the noise emanating from the input port of an amplifier or transistor, as depicted in Fig. 3 [10], [11]. Our simulation program allows inclusion of such measurements, and we have investigated the effect of including one or more such "reverse" measurements among the measurement results to be fit. In terms of the wave-representation, a reverse measurement yields a good determination of X_1. (The expression for T_2 for reverse measurements is, of course, different from that for forward measurements. Both can be found in [2].) Simulation results when a reverse measurement is included are shown in Table 7.The results of Table 7 show a marked improvement in the uncertainty for T_{min}, especially for the two lower-noise

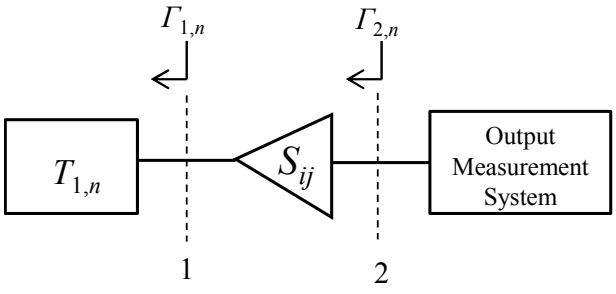

Fig. 3 Configuration for reverse measurements.

Table 7. Simulation results with a reverse measurement.

DUT Input	Bad Frac	$u(G_0)$	$u(T_{min})$ (K)	$u(R_n)$ (Ω)	$u(\lvert\Gamma_{opt}\rvert)$	$u(\varphi_{opt})$
A1						
B	0.35	17.8	4.1	0.091	0.0093	0.61
B+Rev	0.32	15.7	2.2	0.080	0.0094	0.62
A2						
B	0.16	19.6	4.7	0.080	0.0048	0.40
B+Rev	0.17	17.2	2.5	0.076	0.0048	0.40
A3						
B	0.17	2.5	7.5	0.23	0.0044	0.12
B+Rev	0.13	2.3	5.1	0.21	0.0044	0.13

amplifiers, where the improvement is almost a factor of two. There are also small improvements in the G_0 and R_n uncertainties. At first, these results would seem to conflict with the results of [12], [13], which found that the reverse measurement did not improve uncertainties for amplifier noise-parameter measurements. The difference is due to the fact that the earlier results were obtained with the output reflection coefficient $\Gamma_{2,i}$ computed from cascade, whereas the current results assume that they are measured directly, for reasons that will become apparent in the next subsection. When the output reflection coefficients are measured directly, the inclusion of a reverse measurement does improve the uncertainties for the amplifier noise measurements. Unfortunately, a reverse measurement requires a different measurement configuration than the usual forward measurements, and therefore it entails non-negligible additional time and effort.

F. Measurement of Output Reflection Coefficient

One of the options offered by the simulator is the choice of how the output reflection coefficients $\Gamma_{2,i}$ are determined. They can either be measured directly, or they can be computed by cascading the input reflection coefficients $\Gamma_{1,i}$ with the DUT S-parameters $S_{i,j}$. We ran simulations with the same sets of input states (B and B+II, where II represents the four interior points I1, I3, I5, I6) with the output reflection coefficients determined in the two different ways, and Table 8 compares the uncertainties obtained with them measured and computed from cascade. (The results with the output reflection coefficients computed are indicated by (C) following the designation of the input set.)

The results for BadFrac in Table 8 clearly show that measuring the output reflection coefficients is much better than computing them from the other measured quantities, particularly for low-noise devices. As with the inclusion of additional reflective terminations in subsection III.c above, we might think that this effect would disappear if the input

Table 8. Results with output reflection coefficients computed (C), compared to results with them measured.

DUT Input	Bad Frac	$u(G_0)$	$u(T_{min})$ (K)	$u(R_n)$ (Ω)	$u(\lvert\Gamma_{opt}\rvert)$	$u(\varphi_{opt})$
A1						
B	0.35	17.8	4.1	0.091	0.0093	0.61
B(C)	0.83	18.2	4.3	0.14	0.017	0.90
B+II	0.14	18.5	3.8	0.094	0.0095	0.63
B+II(C)	0.90	19.0	3.9	0.084	0.0095	0.58
A2						
B	0.16	19.6	4.7	0.080	0.0048	0.40
B(C)	0.316	19.9	4.7	0.35	0.016	0.68
B+II	0.057	20.4	4.3	0.081	0.0049	0.41
B+II(C)	0.47	21.1	4.6	0.20	0.011	0.50
A3						
B	0.17	2.5	7.5	0.23	0.0044	0.12
B(C)	0.29	2.5	7.7	0.25	0.0071	0.28
B+II	0.042	2.5	6.9	0.23	0.0045	0.13
B+II(C)	0.10	2.6	7.0	0.26	0.0072	0.30

uncertainties for reflection coefficients were smaller. We have run the simulations with the input reflection-coefficient uncertainties reduced by a factor of two, and although the effect is somewhat smaller, the qualitative behavior remains. Even for the smaller uncertainties, it is better to measure rather than compute the output reflection coefficients.

G. Combined Strategies

In the preceding subsections, we considered various possible enhancements of noise-parameter measurement methods, treating them one at a time and comparing the results to those obtained with a base set of input terminations. We now test whether additional improvements are realized by implementing more than one strategy at a time. Based on the results of the preceding subsections, the enhancements that we consider are additional interior points, addition of a cold (*i.e.*, well below ambient) matched load, and inclusion of a reverse measurement. Since it is common practice to use additional interior points, we will compare to the results obtained with the B+II input set (hot and ambient matched loads, four reflective terminations, and four not very reflective terminations). All simulations are done with the output reflection coefficients determined by direct measurement rather than cascade computation. We consider the addition of a cold input source (B+II+c), a reverse measurement (B+II+Rev), and both a cold input source and a reverse measurement (B+II+c+Rev).

Results are tabulated in Table 9. We see that addition of either a cold input source or a reverse measurement leads to significant improvement in the uncertainties for G_0 and T_{min},

Table 9. Results of including multiple enhancements simultaneously.

DUT Input	Bad Frac	$u(G_0)$	$u(T_{min})$ (K)	$u(R_n)$ (Ω)	$u(\lvert\Gamma_{opt}\rvert)$	$u(\varphi_{opt})$
A1						
B+II	0.14	18.5	3.8	0.094	0.0095	0.63
B+II+c	0.15	12.5	1.8	0.074	0.0094	0.63
B+II +Rev	0.17	15.8	2.2	0.078	0.0095	0.63
B+II+c +Rev	0.17	13.1	1.6	0.073	0.0094	0.62
A2						
B+II	0.057	20.4	4.3	0.081	0.0049	0.41
B+II+c	0.064	14.4	2.3	0.069	0.0049	0.41
B+II +Rev	0.079	17.3	2.6	0.075	0.0049	0.41
B+II+c +Rev	0.083	15.2	2.0	0.070	0.0048	0.41
A3						
B+II	0.042	2.5	6.9	.23	0.0045	0.13
B+II+c	0.034	2.1	4.8	.19	0.0045	0.13
B+II +Rev	0.036	2.4	5.3	.22	0.0045	0.13
B+II+c +Rev	0.029	2.1	4.5	.19	0.0045	0.13

and a smaller improvement for R_n. Including both a cold input source and a reverse measurement leads to a small further improvement for T_{min}, but not for G_0 or R_n. Because it is generally easier to add a cold input source than to perform a reverse measurement, the conclusion is that it is certainly worthwhile to add a measurement with a cold input source, but that adding a reverse measurement may not be worth the extra effort.

IV. Summary

We have developed a simulator for noise-parameter measurements and used it to compare uncertainties obtained with several different possible measurement enhancements. The results were obtained on three different amplifiers, with differing properties, and with various different input states, in an attempt to distill general features, not subject to the influence of accidental conspiracies among the detailed characteristics.

Some of the general results can be summarized as follows. The noise temperature of the input hot matched load should be as far from ambient as possible (while still keeping the DUT and output measurement system in their linear operating ranges). It is very helpful to use a cold (cryogenic) input matched load, particularly for low-noise devices. Substituting

a cold load for the hot input load yields some improvements for many amplifiers, but use of a cold load in addition to the hot load yields larger improvements in the uncertainties for all amplifiers considered. The common practice of including interior points (neither reflective nor matched) does indeed lead to better results. The output reflection coefficients should definitely be measured rather than computed by cascade. Additional (beyond four) reflective input terminations do not help and may in fact hurt. Inclusion of a reverse measurement helps, but it requires a different measurement configuration. The practical recommendation that emerges is to add a cold (cryogenic) matched load to the usual set of input terminations; for low-noise devices it will reduce the uncertainty in T_{min} by a factor of about two.

We next plan to perform a similar investigation for on-wafer noise-parameter measurements on transistors.

REFERENCES

[1] J. Randa, "Simulator for amplifier and transistor noise-parameter measurement," *2010 Conference on Precision Electromagnetic Measurements Digest,* pp. 555 – 556, June 2010.

[2] J. Randa, "Uncertainty analysis for noise-parameter measurements at NIST," *IEEE Trans. Instrum. Meas.*, vol. 58, no. 4, pp. 1146 – 1151, April 2009.

[3] G. Caruso and MM. Sannino, "Computer-aided determination of microwave two-port noise parameters," *IEEE Trans. Microw. Theor. Tech.*, vol. 26, no. 11, pp. 639 – 642, 1978.

[4] A.C. Davidson, B.W. Leake, and E. Strid, "Accuracy improvements in microwave noise parameter measurements," *IEEE Trans. Microw. Theor. Tech.*, vol. 37, no. 11, pp. 1973 – 1978, 1989.

[5] S. Van den Bosch and L. Martens, "Improved impedance-pattern generation for automatic noise-parameter determination," *IEEE Trans. Microw. Theor. Tech.*, vol. 46, no. 11, pp. 1673 – 1678, 1998.

[6] J. Randa, "Amplifier and Transistor Noise-Parameter Measurements," in Wiley Encyclopedia of Electrical and Electronics Engineering, edited by John Webster, 2014.

[7] R. Frater and D. Williams, "An active 'cold' noise source," *IEEE Trans. Microw. Theor. Tech.*, vol. MTT-29, no. 4, pp. 344 – 347, April 1981.

[8] L. Dunleavy, M. Smith, S. Lardizabal, A. Fejzuli, and R. Roeder, "Design and characterization of FET based cold/hot noise sources," *IEEEE MTT-S Digest*, pp. 1293 – 1296, May 1997.

[9] P. Buhles and S. Lardizabal, "Design and characterization of MMIC active cold loads," *IEEE MTT-S Digest*, pp. 29 – 32, June 2000.

[10] D. Wait and G. Engen, "Application of radiometry to the accurate measurement of amplifier noise," *IEEE Trans. Instrum. and Meas.*, vol. 40, no. 2, pp. 433 – 437, April 1991; correction: *ibid*, vol. 42, no. 1, p. 78, Feb. 1993.

[11] S. Wedge and D. Rutledge, "Wave techniques for noise modeling and measurement," *IEEE Trans. Microwave Theory & Tech.*, vol. 40, no. 11, pp. 2004 – 2012, Nov. 1992.

[12] J. Randa, "Noise-parameter uncertainties: a Monte Carlo simulation," *J. Res. NIST*, vol. 107, pp. 431 – 444, Sept. 2002; correction: *ibid*, vol. 111, p. 461, Nov. 2006.

[13] J. Randa, T. McKay, S.L. Sweeney, D.K. Walker, L. Wagner, D.R. Greenberg, J. Tao, and G.A. Rezvani, "Reverse noise measurement and use in device characterization," *2006 IEEE Radio Frequency Integrated Circuits (RFIC) Symp. Dig.*, pp. 345 – 348, June 2006.